

RSC Advances



This is an *Accepted Manuscript*, which has been through the Royal Society of Chemistry peer review process and has been accepted for publication.

Accepted Manuscripts are published online shortly after acceptance, before technical editing, formatting and proof reading. Using this free service, authors can make their results available to the community, in citable form, before we publish the edited article. This *Accepted Manuscript* will be replaced by the edited, formatted and paginated article as soon as this is available.

You can find more information about *Accepted Manuscripts* in the [Information for Authors](#).

Please note that technical editing may introduce minor changes to the text and/or graphics, which may alter content. The journal's standard [Terms & Conditions](#) and the [Ethical guidelines](#) still apply. In no event shall the Royal Society of Chemistry be held responsible for any errors or omissions in this *Accepted Manuscript* or any consequences arising from the use of any information it contains.

Synthesis, Characterization and Properties of Telechelic Hybrid Biodegradable Polymers Containing Polyhedral Oligomeric Silsesquioxane (POSS)

M. Jesús Fernández, M. Dolores Fernández, Mónica Cobos

In this work, telechelic POSS-containing inorganic/organic hybrid poly(L-lactic acid) (POSS-PLLA) and ditelechelic POSS-containing hybrid poly(ϵ -caprolactone) (POSS-PCL-POSS) were synthesized by click coupling between alkyne moiety-functionalized POSS and azide end-functionalized PLLA and bis-azide end-functionalized PCL. Characterization of the POSS-containing hybrid polymers was performed using FTIR, ^1H and ^{13}C NMR spectroscopy. The study of the effects of covalent POSS incorporation on the polymer thermal and surface properties was undertaken using differential scanning calorimetry (DSC), thermogravimetric analysis (TGA), and water contact angle measurement. In all synthesized hybrids, glass transition temperature (T_g) increased and crystallization was retarded with the incorporation of POSS moiety at chain ends of PLLA and PCL compared to that of neat homopolymers. Covalent end-capping by POSS disrupted the crystallization of PCL and PLLA. POSS moieties, attached to both ends of PCL, crystallized in the polymer matrix prior to PCL crystallization from the melt. The thermal and thermal oxidative stability of the polymers enhanced significantly after incorporation of the POSS moiety. Static contact angle measurements revealed that the POSS-containing polymers displayed a significant enhancement in surface hydrophobicity.

1. Introduction

The preparation of polyhedral oligomeric silsesquioxanes (POSS)-polymer hybrid materials has received a great deal of attention in recent years due to the observed enhancement of the properties of the organic matrix (increased thermal and oxidation resistance, surface hardening as well as reduced flammability and heat evolution in combustion) upon incorporation of POSS molecules.¹⁻⁶ POSS molecules have a rigid cage-like structures consisting of an inorganic silica like core (Si_8O_{12}) with a 0.53 nm side length that is externally covered by eight organic corner substituents. These organic groups can be inert or reactive, and control the reactivity and the solubility of the POSS molecules.^{4,7,8} The reactive POSS molecules can be easily incorporated into organic polymers via copolymerization employing several polymerization techniques⁹ such as ring-opening polymerization (ROP),¹⁰⁻¹² free radical polymerization^{13,15} and controlled/“living” radical polymerization (CRP),¹⁶ such as atom-transfer radical polymerization (ATRP)¹⁷ and reversible addition-fragmentation

chain transfer polymerization (RAFT).^{18,19} In addition, the covalent binding of the polymer onto the POSS surface can be achieved by reactive grafting approaches, using POSS as a grafting site to initiate chain growth, or grafting POSS to previously synthesized polymer chains. In the first approach, the functionalized POSS core is used to initiate the growth of polymer chains.²⁰ In the second grafting approach, end-functionalized polymer molecules react with complementary functional groups located on the POSS surface to form tethered chains.²¹ Depending on the number of POSS functional groups, a great variety of POSS-polymer architectures can be obtained.²² The POSS moiety can be located at a single end of a polymer chain to form a hemi-telechelic POSS-polymer or at both ends to yield POSS-containing di-telechelic polymer. POSS-containing hybrid block copolymers and star-shaped POSS-containing hybrid polymers have also been synthesized.⁵

The copper catalyzed 1,3-dipolar cycloaddition of azides and terminal alkynes (the so-called “click chemistry” reaction) has been widely used in the preparation of end or pendent functionalized polymers, new monomers and macromonomers

and block copolymers.²³⁻²⁸ This particular reaction is efficient, highly selective, easy to implement and known to be environmental friendly. Some POSS-capped telechelic polymers have been synthesized via copper catalyzed Huisgen cycloaddition reaction.^{5,29}

Aliphatic polyesters have attracted much research interests due to their biodegradability and biocompatibility.^{30,31} Polycaprolactone (PCL) and polylactide (PLA) are among the most used aliphatic polyesters, and owing to their degradability and biocompatibility, they represent interesting candidates for environmentally benign packing materials and for biomedical applications.^{32,33} POSS molecule is also a promising material in biological fields, due to its advantageous properties such as high mechanical property and biodegradability provided by the Si–O–Si bonds.^{34,35} In the latter years, some work has also been carried out on the preparation of POSS-containing telechelic hybrid biopolymers. For example, POSS-capped PCL has been synthesized via ROP using either monohydroxylated or hydroxylated POSS molecules³⁶⁻³⁹ and amino-functionalized POSS as the initiator.^{12,40} POSS molecules have also been incorporated into PLLA to obtain POSS containing PLLA hybrids using ROP initiated by hydroxyl and amino-functionalized POSS.^{12,41} However, with respect to hemitelechelic-POSS PLLA and di-telechelic-POSS PCL obtained by grafting POSS to previously synthesized polymer chains there are not reported studies, thus far.

In this contribution, we report a new preparation of POSS-containing hemi-telechelic poly(L-lactic acid) (PLLA) (POSS-PLLA), and POSS-containing di-telechelic poly(ϵ -caprolactone) (POSS-PCL-POSS) via the Huisgen 1,3-dipolar cycloaddition of azides and alkyne-terminated moieties (“click chemistry” reaction). The new hybrid materials were examined for their thermal properties by both DSC and TGA and the surface properties were observed. One of the important applications of the new nanohybrids is that they can be used as organo-modified POSS nanoparticles to prepare PLLA or PCL based nanocomposites, or nanocomposites made from polymers that are miscible or mechanically compatible with PCL e.g. polyvinyl chloride (PVC), polycarbonate (PC), poly(styrene-co-acrylonitrile) (SAN), poly(acrylonitrile-co-butadiene-co-styrene) (ABS), epoxy resin, nitrocellulose..., in order to promote more favorable POSS-polymer interactions, leading to better dispersion of nanoparticles in the polymer matrix that could enhance the material properties.

2. Experimental section

2.1. Materials

Poly(L-lactic acid) (PLLA) ($M_w = 2000$) was purchased from Polysciences. Polycaprolactone-diol (PCL) ($M_n = 2000$), propiolic acid, p-toluensulfonylchloride (TsCl), *N,N'*-dicyclohexylcarbodiimide (DCC), triethylamine, trimethylamine hydrochloride, sodium azide, copper (II) sulphate pentahydrate ($\text{CuSO}_4(\text{H}_2\text{O})_5$), sodium L-ascorbate, deuterated trichloromethane (CDCl_3) and 1,3-dimethyl-3,4,5,6-tetrahydro-2(1H)-pyrimidinone (DMPU) were obtained from Sigma-Aldrich. Aminopropylheptaisobutyl polyhedral oligomeric

silsesquioxane (APIBOSS) and aminopropylheptaisooctyl POSS (APIOPOSS) were purchased from Hybrid plastics. Methylene chloride (CH_2Cl_2), trichloromethane (CHCl_3), toluene, hexane, tetrahydrofuran (THF), diethylether, methanol and *N,N*-Dimethylformamide (DMF) were obtained from Scharlau. Copper (I) iodide (CuI) and 2,6-lutidine were purchased from Alfa Aesar.

2.2 Polymer synthesis

2.2.1. Synthesis of N-(3-(heptaisobutyl polyhedral oligomeric silsesquioxane) propyl) propiolamide (alkyne-PIBOSS)

To a solution of APIBOSS (2.2 g, 2.5 mmol) and propiolic acid (0.193 g, 2.75 mmol) in dichloromethane (10 mL) was added DCC (0.565 g, 2.75 mmol). The reaction mixture was kept at room temperature for 1 h. Evaporation of the solvent was followed by coevaporation with toluene giving a solid that was dissolved in hexane and then filtered. The filtrate was precipitated in methanol at 0 °C. The resulting product was filtered and dried under vacuum to give 2.3 g of alkyne-PIBOSS, 90% yield.

2.2.2. Synthesis of N-(3-(heptaisooctyl polyhedral oligomeric silsesquioxane) propyl) propiolamide (alkyne-PIOPOSS)

To a solution of APIOPOSS (3.2 g, 2.5 mmol) and propiolic acid (0.193 g, 2.75 mmol) in dichloromethane (10 mL) was added DCC (0.565 g, 2.75 mmol). The reaction mixture was kept at room temperature for 1 h. Evaporation of the solvent was followed by coevaporation with toluene giving a syrup that was dissolved in hexane and then filtered. The filtrate was concentrated by a rotary evaporator and then dried under vacuum to give 3.2 g of alkyne-PIOPOSS, 96% yield.

2.2.3. Synthesis of di-tosylated polycaprolactone (TsO-PCL-OTs)

PCL-diol (6 g, 3 mmol) was dissolved in 10 mL of THF, then triethylamine (10.4 mL, 75 mmol) and trimethylamine hydrochloride (0.143 g, 1.5 mmol) were added. A solution of freshly prepared TsCl (2.85 g, 15 mmol) in 15 mL of THF was slowly added to the above PCL-diol solution at room temperature. After stirring for 1 day the mixture solution was filtered, in order to remove insoluble products. The clear filtrate was precipitated in ethyl ether at 0 °C. The resulting product was filtered and dried under vacuum. The product (4.8 g) was obtained with the yield of 74%.

2.2.4. Synthesis of bis-azide polycaprolactone (N_3 -PCL- N_3)

Sodium azide (0.286 g, 4.4 mmol) was added to a solution of di-tosylated polycaprolactone (5.0 g, 2.2 mmol) in DMF (20 mL). The solution was allowed to stir 24 hours at room temperature. After reaction, insoluble products were filtered and the filtrate was precipitated into hexane at 0 °C. The resulting product, bis-azide polycaprolactone (N_3 -PCL- N_3), was filtered and dried under vacuum. The product (4.1 g) was obtained with the yield of 88%.

2.2.5. Synthesis of *p*-toluenesulfonyl-poly(L-lactic acid) (PLLA-OTs)

PLLA (3.5 g, 1.75 mmol) was dissolved in 10 mL of dichloromethane, then triethylamine (3 mL, 21.5 mmol) and trimethylamine hydrochloride (0.05 g, 0.525 mmol) were added. A solution of freshly prepared TsCl (1 g, 5.25 mmol) in 5 mL of dichloromethane was slowly added to the above PLLA solution at room temperature. After stirring for 1 day the mixture solution was filtered, in order to remove insoluble products. The clear filtrate was precipitated in ethyl ether at 0 °C. The resulting product was filtered and dried under vacuum. The product (3 g) was obtained with the yield of 88%.

2.2.6. Synthesis of azido-poly(L-lactic acid) (PLLA-N₃)

Sodium azide (0.215 g, 3.3 mmol) was added to a solution of *p*-toluenesulfonyl-poly(L-lactic acid) (4.7 g, 2.2 mmol) in DMF (20 mL). The solution was allowed to stir 24 h at 80 °C. After reaction, insoluble products were filtered and the filtrate was precipitated in ethyl ether at 0 °C. The resulting product, azido-poly(L-lactic acid) (PLLA-N₃), was filtered and dried under vacuum. The product (3.4 g) was obtained with the yield of 75%.

2.2.7. Preparation of di-telechelic POSS-containing poly(ϵ -caprolactone) (PIBOSS-PCL-PIOPOSS) via "click" reaction between alkyne-PIBOSS and polycaprolactone bis-azide (N₃-PCL-N₃) catalyzed by CuII/sodium ascorbate

To a solution of alkyne-PIBOSS (0.48 g, 0.51 mmol) and N₃-PCL-N₃ (0.50 g, 0.23 mmol) in DMPU (5 mL) were added a freshly prepared solutions of sodium ascorbate (105 μ L, 0.105 mmol, 1 mol L⁻¹) and copper sulfate pentahydrate in water (42 μ L, 0.021 mmol, 0.5 mol L⁻¹). The solution was stirred at 50 °C for 24 h in the absence of light. The residue was dissolved in dichloromethane and passed through a neutral alumina column to remove copper catalysts. Then the solution was concentrated and precipitated into cold methanol and then the resulting product was washed twice with hexane. The crude product was dissolved in 5 ml of THF, precipitated in methanol and washed with hexane again and dried under vacuum. The product (0.55 g) was obtained with the yield of 80%.

2.2.8. Preparation of di-telechelic POSS-containing poly(ϵ -caprolactone) (PIOPOSS-PCL-PIOPOSS) via "click" reaction between alkyne-PIOPOSS and polycaprolactone bis-azide (N₃-PCL-N₃) catalyzed by CuII/sodium ascorbate

To a solution of alkyne-PIOPOSS (0.67 g, 0.51 mmol) and N₃-PCL-N₃ (0.50 g, 0.23 mmol) in DMPU (5 mL) were added a freshly prepared solutions of sodium ascorbate (105 μ L, 0.105 mmol, 1 mol L⁻¹) and copper sulfate pentahydrate in water (42 μ L, 0.021 mmol, 0.5 mol L⁻¹). The solution was stirred at 50 °C for 24 h in the absence of light. The residue was dissolved in dichloromethane and passed through a neutral alumina column to remove copper catalysts. Then the solution was concentrated and precipitated into cold methanol and then the resulting product was washed twice with hexane. The crude product was dissolved in 5 ml of THF, precipitated in methanol

and washed with hexane again and dried under vacuum. The product (1 g) was obtained with the yield of 90%.

2.2.9. Preparation of di-telechelic POSS-containing poly(ϵ -caprolactone) (PIOPOSS-PCL-PIOPOSS) via "click" reaction between alkyne-PIOPOSS and polycaprolactone bis-azide (N₃-PCL-N₃) catalyzed by CuI

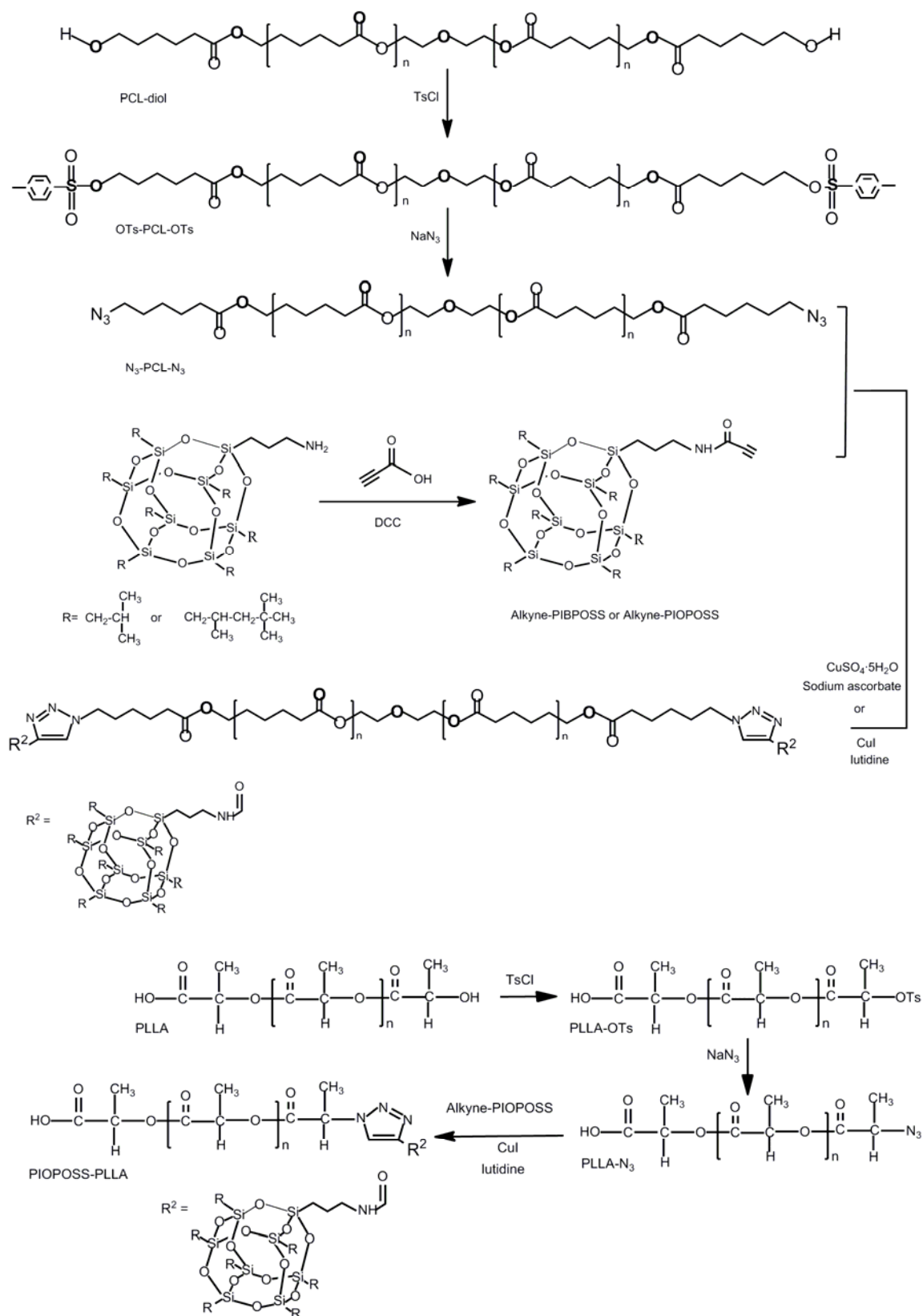
Under a nitrogen atmosphere, alkyne-PIOPOSS (0.80 g, 0.61 mmol), N₃-PCL-N₃ (0.60 g, 0.27 mmol) and 2,6-lutidine (283 μ L, 2.44 mmol) were dissolved in trichloromethane (10 mL). The flask was flushed with nitrogen, frozen and evacuated for three times, after which CuI (0.023 g, 0.122 mmol) was added under nitrogen, and the flask was purged with nitrogen for another 5 min. The reaction was carried out at room temperature for 24 h. After that, the solution was diluted with trichloromethane and passed through a column of neutral alumina to remove the salts of copper. Then the solution was concentrated and precipitated into cold methanol and then the resulting product was washed twice with hexane. The crude product was dissolved in 5 ml of THF, precipitated in methanol and washed with hexane again and dried under vacuum. The product (1 g) was obtained with the yield of 80%.

2.2.10. Preparation of hemi-telechelic POSS-containing poly(L-lactic acid) (PIOPOSS-PLLA) via CuI-catalyzed click coupling

Under a nitrogen atmosphere, alkyne-PIOPOSS (0.63 g, 0.48 mmol), PLLA-N₃ (0.50 g, 0.242 mmol) and 2,6-lutidine (223 μ L, 1.92 mmol) were dissolved in trichloromethane (10 mL). The flask was flushed with nitrogen, frozen and evacuated for three times, after which CuI (0.018 g, 0.096 mmol) was added under nitrogen, and the flask was purged with nitrogen for another 5 min. The reaction was carried out at room temperature for 24 h. After that, the solution was diluted with trichloromethane and passed through a column of neutral alumina to remove the salts of copper. Then the solution was concentrated and precipitated into cold methanol and then the resulting product was washed twice with hexane. The crude product was dissolved in 5 ml of THF, precipitated in methanol and washed with hexane again and dried under vacuum. The product (0.5 g) was obtained with the yield of 80%.

2.3. Characterization

Fourier-transform infrared (FTIR) measurements were carried out on a Thermo Scientific Nicolet iN10 FTIR spectrometer at room temperature. ¹H and ¹³C nuclear magnetic resonance (NMR) spectra were recorded on a 300 MHz Bruker DSX-300 spectrometer using tetramethylsilane (TMS) as an internal chemical shift standard and CDCl₃ as the internal standard for ¹³C NMR. Differential scanning calorimetry analyses (DSC) were performed on a TA instruments TA-DSC Q2000 at a heating rate of 10 °C min⁻¹ under nitrogen atmosphere. PCL and POSS-PCL-POSS nanohybrids were first heated from room temperature to 100 °C, held for 5 min to erase previous thermal history and then were cooled to -100 °C at 10 °C min⁻¹ and held for 3 min. After that, the samples were reheated from -100 °C to 100 °C at 10 °C min⁻¹. The glass transition, crystallization and



Scheme 1 Synthetic route for the synthesis of POSS-PCL-PCL and POSS-PLLA hybrids.

melting temperatures were taken as the mid point of the capacity change and the maximum of exothermic and endothermic transition, respectively. PLLA and PLLA-POSS nanohybrid samples were weight to be in the range 5-6 mg, and were first heated from room temperature to 170 °C and held in the molten state for 5 min to erase the thermal history. Then, the samples were cooled to 0 °C at 10 °C min⁻¹ and held 3 min, and again heated to 170 °C at 10 °C min⁻¹. Finally, after being cooled to 0 °C at the highest attainable cooling rate the samples were heated again to 170 °C at 10 °C min⁻¹. Thermogravimetry analyses were performed on a TA instruments His Res TG-Q-500 under nitrogen and oxygen atmosphere from ambient temperature to 750 °C at a heating rate of 10 °C min⁻¹. The thermal degradation temperature was taken as the onset temperature at which 5 % of weight loss occurs. Static contact angle was measured by using the sessile drop technique placing a droplet of deionized water on the surface of the various substrates using a digital goniometer equipped with a dispensing needle (Dataphysics Contact Angle System OCA).

3. Results and discussion

3.1. Synthesis

Telechelic hybrid biodegradable polymers containing POSS were synthesized using Cu(I)-catalyzed Huisgen [3+2] cycloaddition “click chemistry” between alkyne-functionalized POSS and azido-functionalized PCL and PLLA. Two amino-derivative POSS were converted to alkyne-functionalized POSS. In parallel, hydroxyl end groups of polycaprolactone-diol and PLLA were substituted by azide groups to generate the azido derivative polymers. Finally, azido-terminated polymer chains were reacted with alkyne-functionalized POSS molecules through “click chemistry” to produce telechelic POSS containing hybrid polycaprolactone (POSS-PCL-POSS) and poly(L-lactic acid) (POSS-PLLA). The synthetic process is summarized in Scheme 1.

3.1.1. Synthesis of alkyne-terminated POSS

Alkyne-POSS (alkyne-PIBPOSS and alkyne-PIOPOSS) were prepared by amide formation between amino-POSS (APIBPOSS, a white crystalline powder, and APIOPOSS, a pale yellow viscous liquid) and a carboxylic acid containing alkyne moiety (2-propynoic acid) with stoichiometric amounts of dicyclohexylcarbodiimide (DCC) as coupling reagent and methylene chloride as solvent. The amide formation was confirmed by FTIR. FTIR spectra of alkyne-PIBPOSS and alkyne-PIOPOSS compared to those of APIBPOSS and APIOPOSS (Fig.1) displayed two new bands at 3310 cm⁻¹ and 2120 cm⁻¹, assigned to the stretching vibration of ≡C-H and C≡C of alkynes, respectively. In addition, another two new bands appeared at 1640 cm⁻¹ and 1530 cm⁻¹ due to the formation of the amide groups, stretching vibration of C=O and bending vibration of N-H, respectively. The ¹H NMR spectra of APIBPOSS, APIOPOSS, alkyne-PIBPOSS and alkyne-PIOPOSS

are shown in Fig. 2. The ¹H NMR spectra of alkyne-PIBPOSS and alkyne-PIOPOSS compared to that of APIBPOSS and APIOPOSS showed the shift of the signal of methylene protons (-CH₂NH₂-) from 2.67 ppm to 3.25 ppm assigned to the resonance of methylene protons (-CH₂NHCO-).

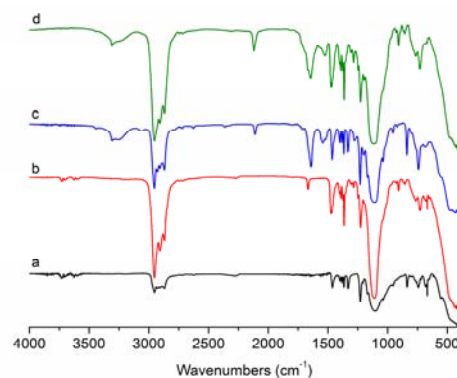


Fig.1 FTIR spectra of (a) APIBPOSS, (b) APIOPOSS, (c) alkyne-PIBPOSS, and (d) alkyne-PIOPOSS

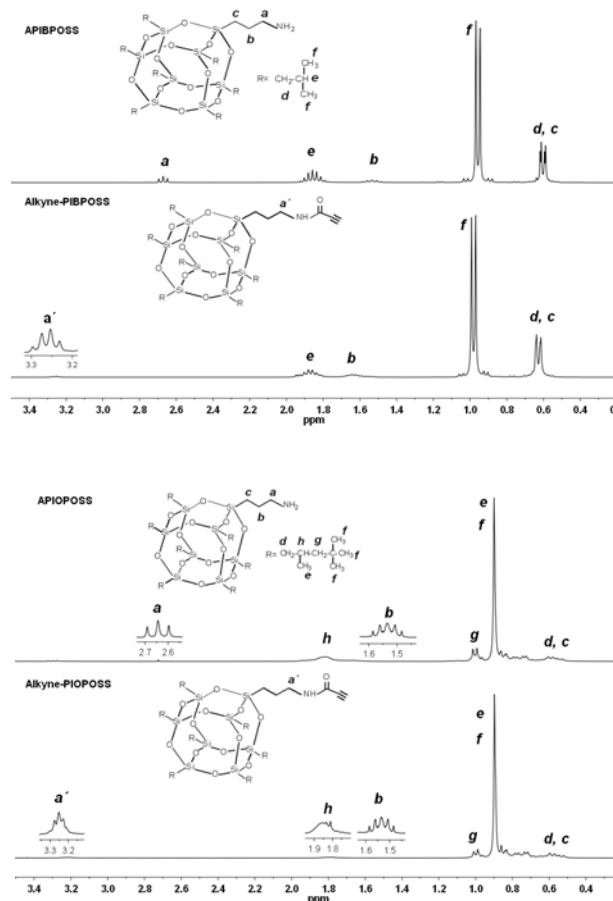


Fig. 2 ¹H NMR spectra of APIBPOSS, alkyne-PIBPOSS, APIOPOSS and alkyne-PIOPOSS.

3.1.2. Synthesis of azido-PCL

The conversion of PCL-diol into azido-PCL was achieved in two steps. First, tosylation of hydroxyl end groups of PCL-diol by *p*-toluenesulfonylchloride was carried out for the purpose of making a leaving group. The reaction was performed in THF using triethylamine as base and catalytic amounts of trimethylamine hydrochloride.⁴² The FTIR spectrum of the tosylated PCL compared to that of PCL-diol (Fig. 3) showed the complete disappearance of the signal at around 3500 cm⁻¹, assigned to the stretching vibration of O-H of alcohols, and two new peaks at 1600 and 680 cm⁻¹ assigned to the backbone vibrations (C=C stretching) and C-H bending of the benzene ring, respectively. Fig. 4 displays the ¹H NMR spectra of PCL, tosylated PCL and bis-azide PCL. The PCL-diol spectrum exhibited the signals originating from the methine protons in the main chain and those at the hydroxylic end units. The ¹H NMR spectrum of the tosylated PCL showed the signals at δ = 2.45 ppm, 7.30 ppm and 7.74 ppm assigned to methyl and aromatic protons of tosylo groups, respectively, and the disappearance of the signal at 3.59 ppm assigned to the methylene protons of terminal CH₂-OH in PCL-diol. The ¹³C NMR spectrum of the tosylated PCL (Fig. 5) showed the disappearance of the peak at 62.7 ppm assigned to the methylene carbon of terminal CH₂-OH in PCL-diol and new signals at 70.2 ppm assigned to terminal methylene carbon linked to tosylo group, 127.8 ppm, and 129.8 ppm corresponding to aromatic carbons of tosylo groups. These results confirmed that di-tosylated PCL was obtained. The terminal tosylo groups were transformed into azide groups to produce the bis-azide PCL, N₃-PCL-N₃, via nucleophilic substitution. The reaction was carried out in DMF, using an excess of sodium azide, at room temperature. FTIR was used to characterize the terminal azido groups. Compared to the FTIR spectrum of di-tosylated PCL, a new band at 2095 cm⁻¹ appeared in the spectrum of N₃-PCL-N₃ (Fig. 3), which is assigned to stretching vibration of terminal azido groups. The band at 1600 and 680 cm⁻¹, assigned to the backbone and bending vibrations of the benzene ring, disappeared.

In addition, ¹H and ¹³C NMR were used to confirm the total substitution of tosylo groups by N₃-counterpart. The ¹H NMR spectrum of azido-PCL (Fig. 4) showed the complete disappearance of the signals at 7.30 ppm and 7.74 ppm (corresponding to the aromatic protons), and a new signal peak appeared at 3.25 ppm, which is ascribed to the methylene adjacent to terminal azide group (CH₂-N₃). The ¹³C NMR spectrum of N₃-PCL-N₃ (Fig. 5) showed the total disappearance of the peaks at 70.2 ppm, 127.8 ppm and 129.8 ppm assigned to terminal methylenic carbons and aromatic carbons of tosylo groups, respectively, and the appearance of a new peak at 51.2 ppm corresponding to the terminal methylene moiety linked to azido group. These results confirmed the total substitution of tosylo groups by azide.

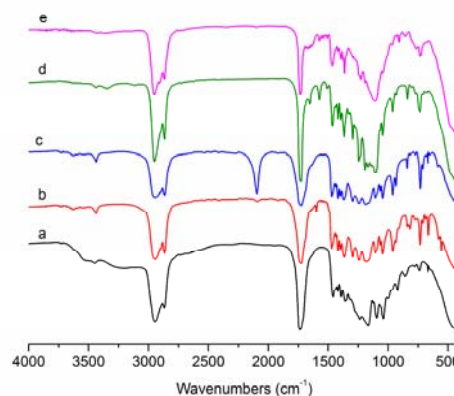


Fig. 3 FTIR spectra of (a) PCL-diol, (b) di-tosylated PCL, (c) bis-azide PCL, (d) PIBOSS-PCL-PIBOSS, and (e) PIOPOSS-PCL-PIOPOSS.

3.1.3. Synthesis of azido-poly(L-lactic acid)

The conversion of PLLA into azido-PLLA was also achieved in two steps. First, tosylation of hydroxyl end groups of PLLA by *p*-toluenesulfonylchloride was carried out for the purpose of making a leaving group. The reaction was performed in dichloromethane using triethylamine as base and catalytic amounts of trimethylamine hydrochloride. Comparing the FTIR spectra of PLLA and tosylated PLLA (Fig. 6) it was observed that a small new peak appeared at 1600 cm⁻¹ assigned to the backbone vibrations (C=C stretching) of the benzene ring.

The ¹H NMR spectra of PLLA, tosylated PLLA and azido-PLLA are shown in Fig. 7. In the PLLA spectrum, two intense signals located at 1.57 ppm assigned to the methyl protons in the main chain -CH(CH₃)-COO-, and at 5.16 ppm assigned to the methine protons -CH(CH₃)-COO- in the main chain were observed. Moreover, two weak signals at 4.34 ppm and 4.12 ppm which were assigned respectively to the methine protons at the hydroxylic and the carboxylic end units were observed. The ¹H NMR spectrum of the tosylated PLLA (Fig. 7) showed the signals at δ = 2.44 ppm, 7.30 ppm and 7.74 ppm assigned to methyl and aromatic protons of tosylo groups, respectively, the disappearance of the signal at 4.34 ppm assigned to the methine protons of terminal CH-OH in PLLA and the appearance of a new band at 5.16 ppm assigned to the methine protons of terminal CH-OTs. The ¹³C NMR spectra of original PLLA and tosylated PLLA are shown in Fig. 8. The ¹³C NMR spectrum of PLLA showed the intense signals due to the carbonyl carbons at 169.7 ppm, the methine and the methyl carbons in the repetitive central units at 69.13 ppm and 16.73 ppm, respectively. The contribution of the hydroxylic end units gave rise to the weak signal at 66.83 ppm assigned to methine carbons of these chain end groups and the carboxylic end units to the signal at 65.80 ppm due to methine carbons.

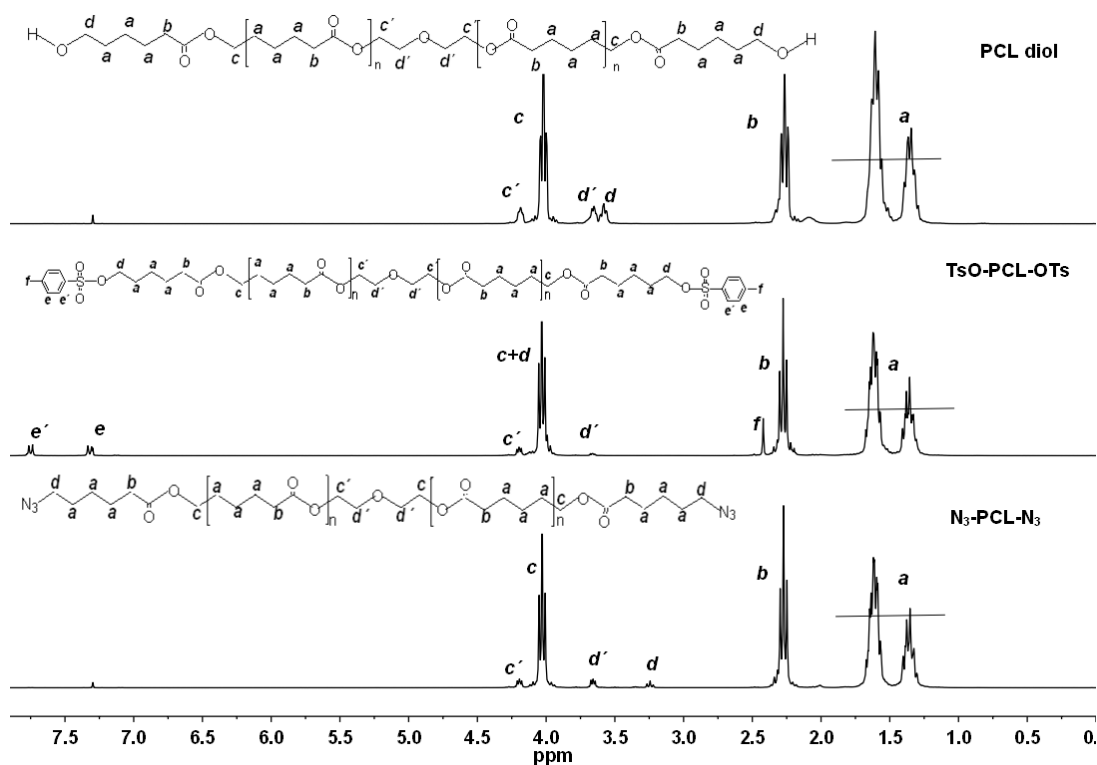


Fig. 4 ^1H NMR spectra of PCL-diol, di-tosylated-PCL and bis-azide-PCL.

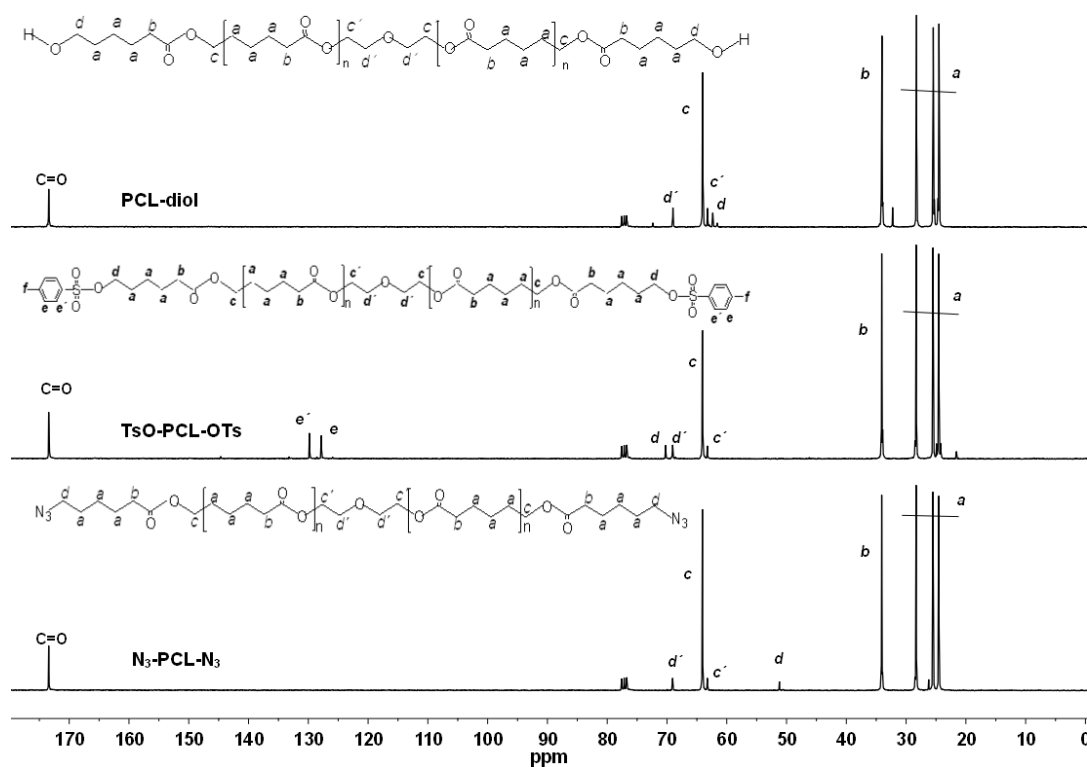


Fig. 5 ^{13}C NMR spectra of PCL-diol, di-tosylated-PCL, and bis-azide-PCL.

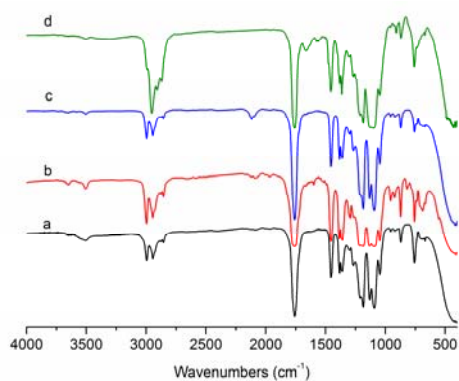


Fig. 6 FTIR spectra of (a) PLLA, (b) tosylated-PLLA, (c) azide-PLLA and (d) PEOSS-PLLA.

The ^{13}C NMR spectrum of the tosylated PLLA (Fig. 8) showed the disappearance of the peak at 66.83 ppm assigned to methine carbon at the hydroxylic end units in PLLA and new signals at 73.42 ppm assigned to methine carbon of terminal CH-OTs, 129.8 ppm, and 133.5 ppm corresponding to aromatic

carbons of tosyl groups. These results confirmed that tosylated PLLA was obtained. The terminal tosyl groups were transformed into azide groups to produce azido-PLLA, PLLA- N_3 , via nucleophilic substitution. The reaction was carried out in DMF, using an excess of sodium azide, at 80 °C. FTIR was used to characterize the terminal azido groups. Compared to the FTIR spectrum of tosylated PLLA, a new band at 2095 cm^{-1} appeared in the spectrum of PLLA- N_3 (Fig. 6), which is assigned to stretching vibration of terminal azido groups. In addition, ^1H and ^{13}C NMR were used to confirm the total substitution of tosyl groups by N_3 -counterpart. The ^1H NMR spectrum of azido-PLLA (Fig. 7) showed the complete disappearance of the signals at 7.30 ppm and 7.74 ppm corresponding to the aromatic protons, and a new signal appeared at 2.58 ppm, which is ascribed to the methine adjacent to terminal azide group (CH-N_3). The ^{13}C NMR spectrum of PLLA- N_3 (Fig. 8) showed the total disappearance of the peak at 73.42 ppm assigned to methine carbon of terminal CH-OTs and the appearance of a new peak at 57.10 ppm corresponding to the terminal methine moiety linked to azido group. These results confirmed the total substitution of tosyl groups by azide.

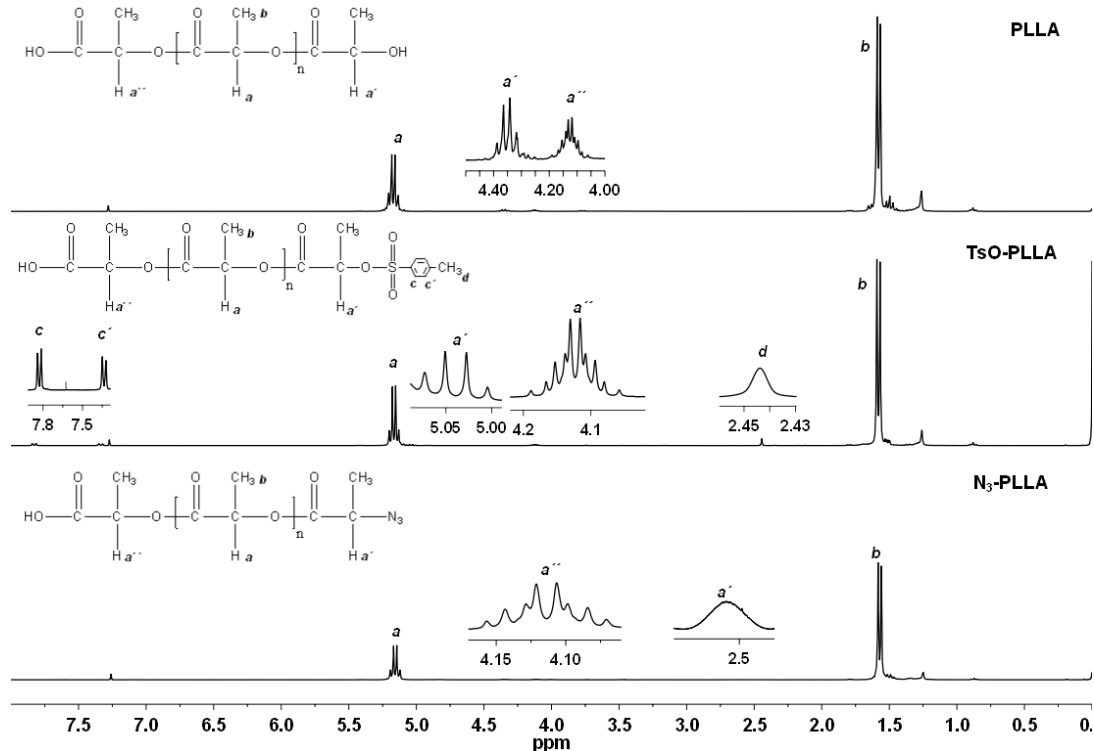


Fig. 7 ^1H NMR spectra of PLLA, tosylated-PLLA and azide-PLLA.

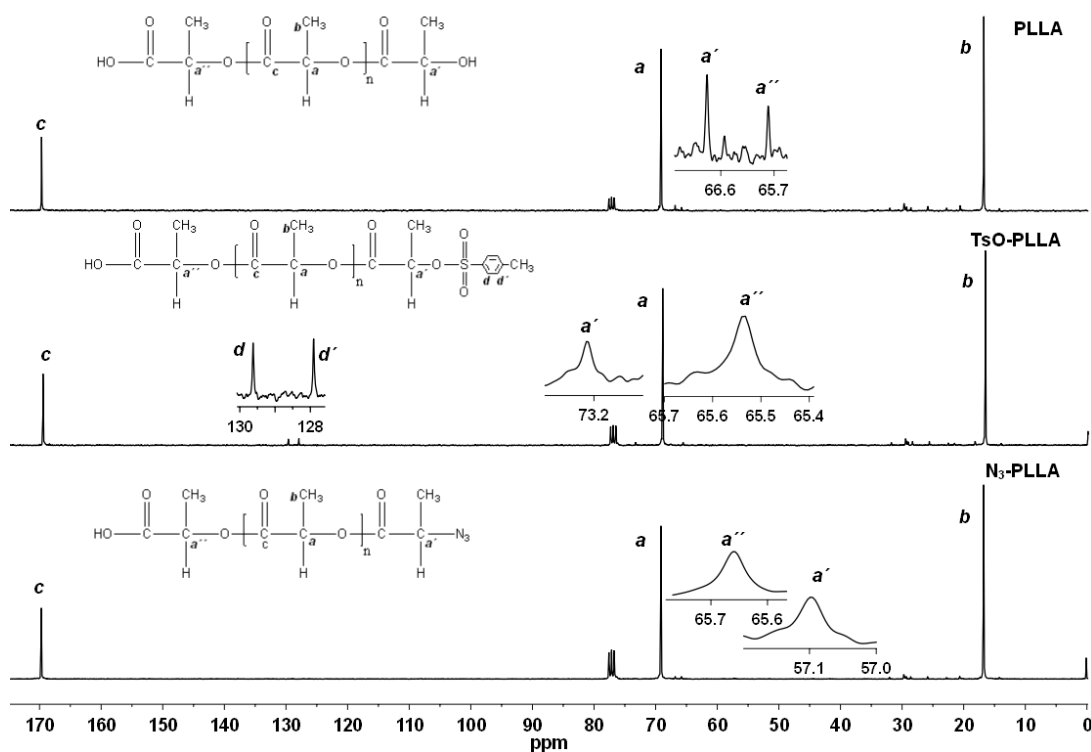


Fig. 8 ^{13}C NMR spectra of PLLA, tosylated-PLLA and azide-PLLA.

3.1.4. Synthesis of telechelic hybrid PCL and PLLA containing POSS

The di-telechelic POSS-containing poly(ϵ -caprolactone) (POSS-PCL-POSS) was obtained via a reaction of alkyne-POSS and bis-azide PCL under click reaction conditions using different catalysts.

The click cycloaddition between N_3 -PCL- N_3 and alkyne-PIBPOSS or between N_3 -PCL- N_3 and alkyne-PIOPOSS was carried out at 50 °C for 24 h using Cu(II) sulfate and sodium ascorbate as catalyst in the absence of UV light (in order to prevent the photodegradation of sodium ascorbate) and DMPU as solvent. To complete the coupling reaction a total of ~ 2.2 eq amounts of alkyne-POSS compared to that of N_3 -PCL- N_3 was used. This excess of alkyne-POSS was removed after the reaction via a washing step with hexane. PIBPOSS-PCL-PIBPOSS and PIOPOSS-PCL-PIOPOSS were characterized by FTIR, ^1H and ^{13}C NMR analyses. The FTIR spectra of POSS-PCL-POSS (Fig. 3) compared to that of azido-PCL showed that the band at 2095 cm^{-1} due to the azide stretching vibration disappeared completely and the appearance a new band at 1107 cm^{-1} , which is assigned to the stretching vibration of Si-O-Si. In addition, the ^1H NMR spectra of POSS-PCL-POSS (Fig. 9) showed the total disappearance of the signal at 3.25 ppm, assigned to the resonance of the methylene adjacent to terminal azide group of N_3 -PCL- N_3 and to the methylene protons

covalently linked to amide groups of alkyne-POSS ($-\text{CH}_2\text{NHCO}-$). Two more signals appeared in the ^1H NMR spectrum of the hybrid materials, one at 8.03 ppm corresponding to the proton of the triazole ring, and the other at 4.38 ppm corresponding to the methylene protons adjacent to the triazole ring. In addition, in the ^1H NMR spectrum of PIBPOSS-PCL-PIBPOSS the signals of the characteristic protons derived from APIBPOSS appeared at 0.61, 0.97 and 1.87 ppm, and in the spectrum of PIOPOSS-PCL-PIOPOSS those from APIOPOSS at 0.61, 0.90 and 1.82 ppm.

Finally, in ^{13}C NMR spectra of POSS-PCL-POSS (Fig. 10) new peaks appeared at 160.36, 143.89, 125.01 and 50.73 ppm assigned to the carbonyl carbon adjacent to the triazole ring, carbons of the triazole ring and methylene carbon adjacent to N of triazole ring, respectively.

The click cycloaddition of azide-PCL-azide/alkyne PIOPOSS was also performed at room temperature for 24 h using CuI/lutidine as catalyst and trichlorometane as solvent. To complete the coupling reaction a total of ~ 2.3 eq amounts of alkyne-POSS compared to that of N_3 -PCL- N_3 was used. FTIR, ^1H and ^{13}C NMR characterizations confirmed that click reaction successfully took place between azide-PCL-azide and alkyne PIOPOSS under those conditions.

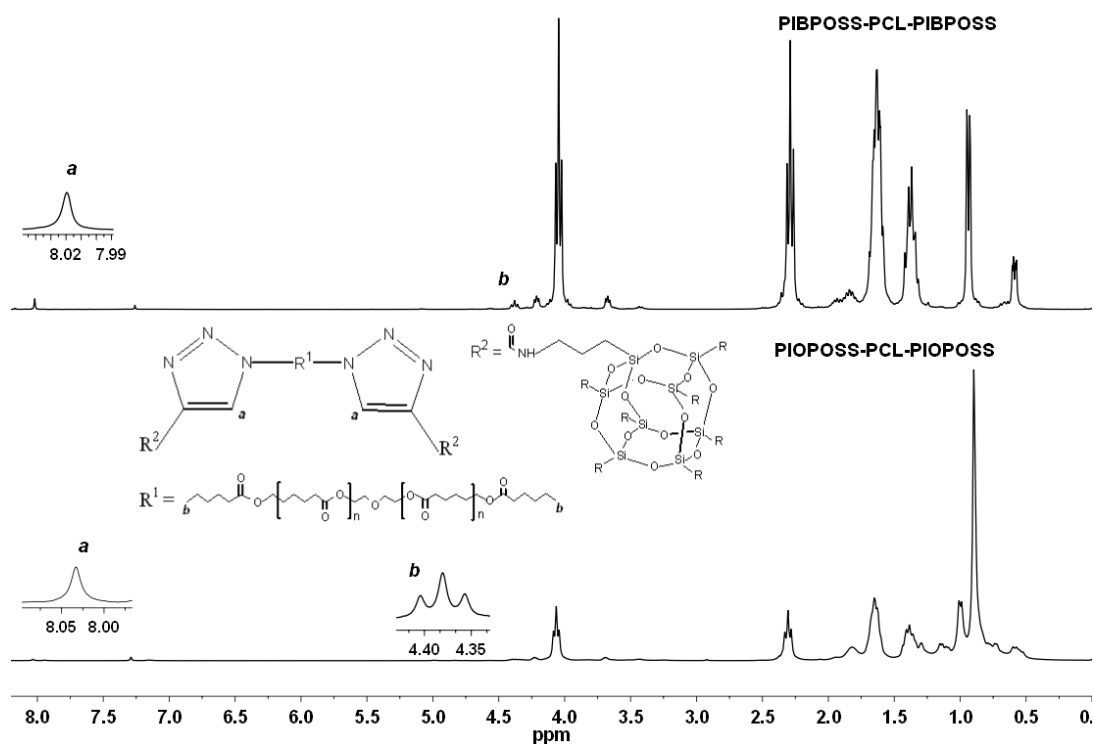


Fig. 9 ^1H NMR spectra of PIBOSS-PCL-PIBOSS and PIVOSS-PCL-PIOVOSS.

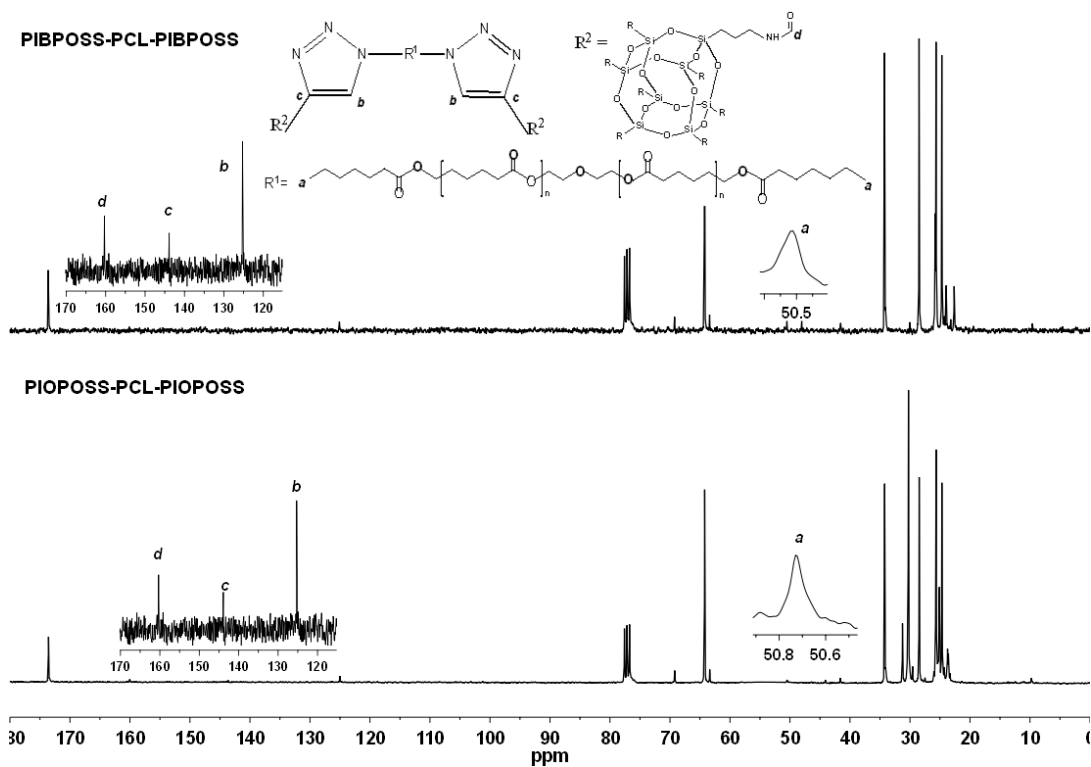


Fig. 10 ^{13}C NMR spectra of PIBOSS-PCL-PIBOSS and PIVOSS-PCL-PIOVOSS.

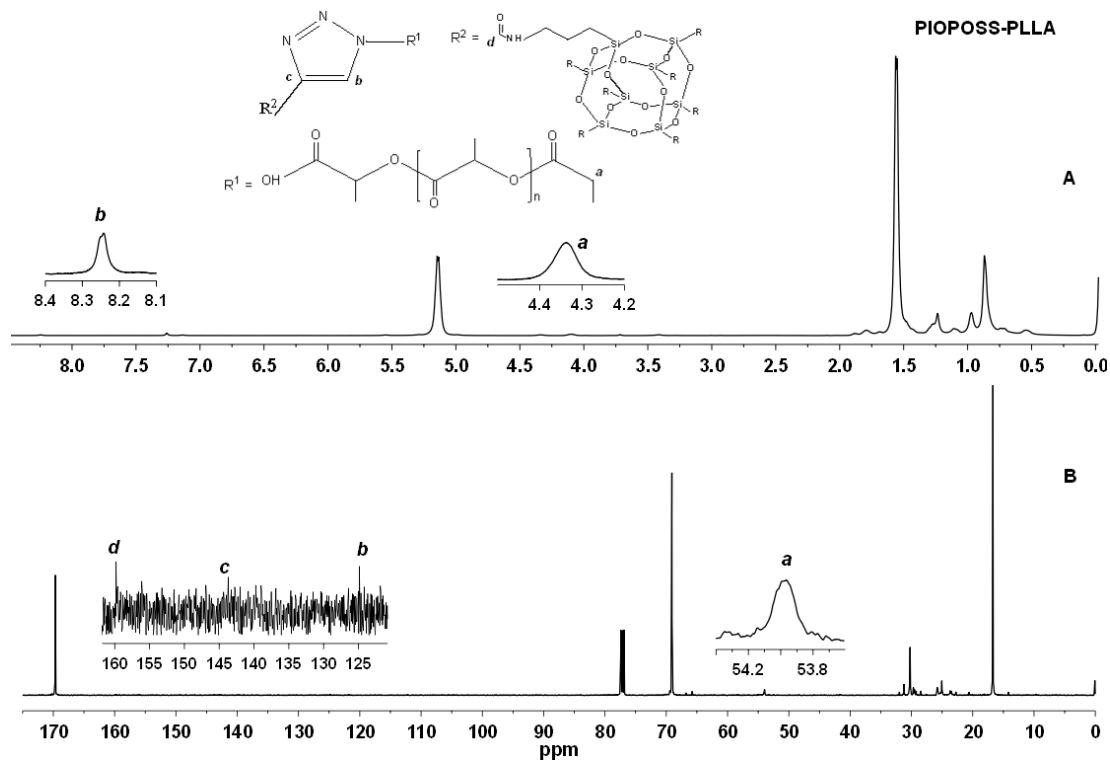


Fig. 11 ^1H NMR and ^{13}C NMR spectra of PIOPOSS-PLLA.

The hemi-telechelic POSS-containing poly(L-lactic acid) (PIOPOSS-PLLA) was obtained via a reaction of alkyne-POSS and azido-PLLA under click reaction conditions. The click cycloaddition between PLLA- N_3 and alkyne-PIOPOSS was carried out at room temperature for 24 h using CuI/lutidine as catalyst and trichlorometane as solvent. To complete the coupling reaction a total of ~ 2 eq amounts of alkyne-PIOPOSS compared to that of PLLA- N_3 was used. This excess of alkyne-POSS was removed after the reaction via a washing step with hexane. PIOPOSS-PLLA was characterized by FTIR, ^1H and ^{13}C NMR analyses. The FTIR spectrum of PIOPOSS-PLLA (Fig. 6) compared to that of azido-PLLA showed that the band at 2095 cm^{-1} due to the azide stretching vibration disappeared completely and the appearance of a new band at 1107 cm^{-1} , which is assigned to the stretching vibration of Si-O-Si. In addition, the ^1H NMR spectrum of PIOPOSS-PLLA (Fig. 11) showed the total disappearance of the signals at 2.58 ppm and 3.25 ppm assigned to the resonance of the methylene adjacent to terminal azide group of PLLA- N_3 and to the methylene protons covalently linked to amide groups of alkyne-POSS ($-\text{CH}_2\text{NHCO}-$), respectively. Two more signals appeared in the ^1H NMR spectrum of the hybrid materials, one at 8.27 ppm corresponding to the proton of the triazole ring, and the other at 4.37 ppm corresponding to the methylene protons adjacent to the triazole ring. In addition, in the ^1H NMR spectrum of PIOPOSS-PLLA the signals of the characteristic protons

derived from APIOPOSS appeared at 0.61, 0.90 and 1.82 ppm. Finally, in ^{13}C NMR spectrum of POSS-PLLA (Fig. 11) new peaks appeared at 159.81, 143.70, 125.03 and 53.96 ppm assigned to the carbonyl carbon adjacent to the triazol ring, carbons of the triazole ring and methylene carbon adjacent to N of triazole ring, respectively.

3.2. Thermal properties

3.2.1. Thermal transitions

DSC measurements were conducted to determine the thermal transitions of the polymer samples and to study the effects of POSS incorporation on these transitions. First cooling and second heating scans for APIBPOSS, PCL and POSS-PCL-POSS hybrids are shown in Fig. 12. Table 1 summarizes the DSC results for these samples. During the second heating (Fig. 12 A down), APIBPOSS had a melting endotherm at $52.9\text{ }^\circ\text{C}$ with a heat of fusion of 19.1 J/g . PCL (Fig. 12 B down) and PIBPOSS-PCL-PIBPOSS (Fig. 12 C down) showed an endothermic peak due to the melt of PCL crystalline phase, PCL exhibited a double melting transition at 43.8 and $49.5\text{ }^\circ\text{C}$ with a total heat of fusion of 81.9 J/g ; while in the thermogram of the hybrid only a single melting endotherm was observed at $47.3\text{ }^\circ\text{C}$ with heat of transition of 40 J/g . However, an additional very weak melting transition was observed for the

hybrid at 89.1 °C with a heat of fusion of 2.2 J/g, relating to the melting of POSS crystallites present in the hybrid. The POSS-based T_m increased, and the POSS-based heat of fusion decreased dramatically as compared to that of pure APIBPOSS. On the other hand, in the second heating thermogram of PIVOPOSS-PCL-PIOPOSS in addition to a single melting endotherm at 44.5 °C, an exothermic peak at 1.1 °C was observed due to the cold crystallization of PCL during heating. Moreover, it was observed that the incorporation of POSS molecules into PCL increased the glass transition temperature by around 5 °C. The rigid cage-like structure of POSS molecules restricts polymer chain motion, thus rising T_g . During cooling (Fig. 12 up), pure APIBPOSS exhibited a crystallization peak at 46.1 °C with a heat of transition of 18.5 J/g, while PCL and PIBPOSS-PCL-PIBPOSS showed an exothermic peak due to the melt crystallization of PCL at 26.3 and 21.5 °C, respectively, with heat of crystallization of 80.2 and 32.7 J/g, respectively. This result indicates that the incorporation of POSS has a retardant effect on the crystallization of PCL due to the confinement effect. However, PIVOPOSS-PCL-PIOPOSS did not exhibit melt crystallization. Fig. 12 C revealed that, for PIBPOSS-PCL-PIBPOSS hybrid, in addition to the crystallization of PCL phase, and additional exothermic peak can be observed at 70.9 °C, with heat of transition of 3.1 J/g due to the POSS phase. POSS-based T_c

increased and the POSS-based heat of crystallization decreased drastically as compared to that of pure POSS. POSS moiety crystallized prior PCL, and thus PCL crystallization have been confined between preexisting POSS crystals. On the other hand PCL accelerated the crystallization of POSS moiety.

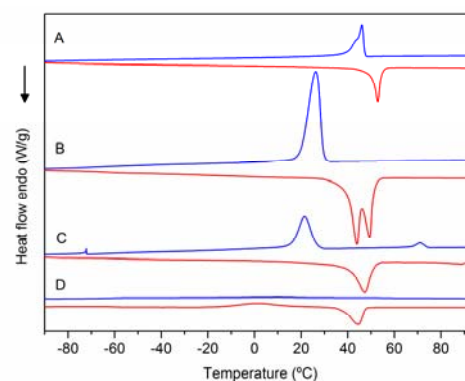


Fig. 12 DSC thermograms of (A) APIBPOSS, (B) PCL, (C) PIBPOSS-PCL-PIBPOSS, and (D) PIVOPOSS-PCL-PIOPOSS. Down: second heating scan. Up: cooling scan.

Table 1. DSC data for APIBPOSS, APIOPOSS, PCL, PLLA and hybrid PCL and PLLA

Sample	Polymer					POSS			
	T_g (°C)	T_c (°C)	T_m (°C)	ΔH_c (J/g)	ΔH_m (J/g)	T_c (°C)	T_m (°C)	ΔH_c (J/g)	ΔH_m (J/g)
APIBPOSS						46.1	52.9	18.5	19.1
PCL	-64.8	26.3	43.8	80.2	81.9				
			49.5						
PIBPOSS-PCL-PIBPOSS	-59.7	21.5	47.3	32.7	40.0	70.9	89.1	3.1	2.2
PIOPOSS-PCL-PIOPOSS	-60.8	1.1	44.5	10.6	16.1				
PLLA	13.5 ^b	108.1 ^a	138.1 ^b	30.7 ^a	35.0 ^b				
	39.0 ^c	73.5 ^c	147.1 ^b						
			147.1 ^c						
PIOPOSS-PLLA	43.4 ^b	89.6 ^a	146.8 ^b	17.0 ^a	26.7 ^b				
	46.3 ^c	90.1 ^c	146.4 ^c						

^a Cooling rate 10 °C/min. ^b Heating after cooling at 10 °C/min. ^c Heating after fast cooling.

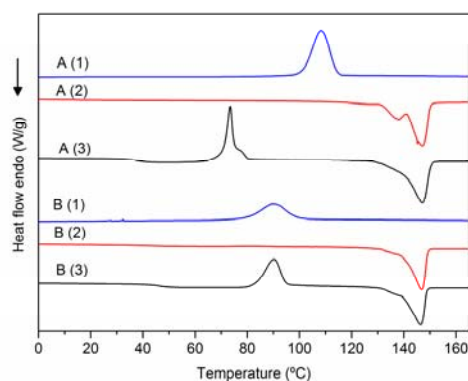


Fig. 13 DSC thermograms of (A) PLLA, and (B) PIOPOSS-PLLA. Down: second heating scan after being cooled at slow (A2, B2) and high cooling rate (A3, B3). Up: cooling scan.

POSS-PCL-POSS hybrids exhibited reduced PCL-based ΔH_c and ΔH_m values compared to the homopolymer, indicating that the incorporation of POSS disrupts the formation of PCL crystallites. Furthermore, PIBPOSS-PCL-PIBPOSS displayed reduced POSS-based ΔH_c and ΔH_m values compared to the pure APIBPOSS, indicating that PCL disrupts the formation of POSS crystallites. As a conclusion, the incorporation of POSS moiety gave rise to less ordered crystals of PCL and subsequently lower melting temperatures and heats of fusion. Fig. 13 compares the thermograms of PLLA and POSS-PLLA hybrid, and the DSC results for these samples are summarized in Table 1. In this case, DSC measurements were performed to determine the cooling rate dependence of the crystallization transition. In the second heating thermogram of the products after being cooled at 10 °C min^{-1} (Fig. 13 curves A2 and B2), it was observed that the incorporation of POSS molecules into PLLA increased the glass transition temperature by around 30 °C . This increase is attributed to a decrease in the mobility of the PLLA segments because of their attachment to the POSS core. Moreover, these second heating DSC traces of PLLA and POSS-PLLA hybrid showed additional endothermic peaks due to the melt of PLLA crystalline phase. PLLA exhibited a double melting transition at 138.1 and 147.1 °C ; while only a single melting endotherm at 146.8 °C was observed in the thermogram of the hybrid. With regards of the melting endotherm, the POSS-PLLA hybrid exhibited reduced ΔH_m value compared to the homopolymer, indicating that the incorporation of POSS disrupts the formation of PLLA crystallites. During the first cooling DSC curves of PLLA and its hybrid (Fig. 13 curves A1 and B1) an exothermic peak due to the melt crystallization of polymer chains at 108.1 and 89.6 °C , respectively, was observed, indicating that the incorporation of POSS retards the crystallization of PLLA. Furthermore, the POSS-PLLA hybrid exhibited reduced ΔH_c value compared to the homopolymer. In the heating thermograms of the products after being cooled at high cooling rate (Fig. 13 curves A3 and B3), it was observed exothermic peaks due to the cold crystallization of PLLA and its hybrid and melting endotherms for both the hybrid and the

pure polymer. The hybrid exhibited increased T_c value as compared to PLLA, indicating once again that the POSS incorporation has a retardant effect on the crystallization of PLLA. With regards to the influence of heating rate on crystallization of polymer samples, the hybrid was not influenced by the cooling rate, while the pure PLLA was greatly influenced as can be seen from data of Table 1. Furthermore, the thermal history of the material greatly influenced the glass transition of PLLA, T_g value increased from 13.5 °C for the slow cooling rate to 39.0 °C for the fast cooling rate. However, the glass transition of the POSS-PLLA hybrid was only slightly affected by the thermal history.

It can be concluded that the incorporation of POSS to the ends of the PLLA chains resulted in less ordered crystals and subsequently lower melting temperatures and heats of fusion.

3.2.2. Thermal stability

The thermal behaviour of the nanohybrids was studied by TG in both inert and oxidative atmosphere, in order to investigate the effects of covalently tethered POSS nanoparticles on the thermal stability of the telechelic polymers. The thermogravimetric curves evidenced different behaviors in the studied environments. The TG and DTG curves for pure POSS (APIBPOSS and APIOPOSS), PCL and nanohybrids (PIBPOSS-PCL-PIBPOSS and PIOPOSS-PCL-PIOPOSS) in nitrogen and oxygen atmosphere are reported in Figs. 14-15, and 16-17, respectively.

The temperatures at 5% weight loss (T_5), the temperatures of DTG peaks (T_{max}), which are the temperatures at maximum weight loss rate, and the values of the residues obtained after complete temperature scan are reported in Table 2. In N_2 atmosphere, the weight loss took place in a single step for APIBPOSS falling in the $165\text{--}270\text{ °C}$ temperature range, while APIOPOSS showed a two-step decomposition process in the $205\text{--}540\text{ °C}$ temperature range. The homopolymer PCL showed a two-step decomposition process in the two used atmosphere, falling in the $215\text{--}470\text{ °C}$ temperature range in nitrogen, and in $200\text{--}500\text{ °C}$ temperature range in oxygen. The nanohybrids, PIBPOSS-PCL-PIBPOSS and PIOPOSS-PCL-PIOPOSS, showed a single step decomposition process in N_2 atmosphere falling in the $340\text{--}415\text{ °C}$ and $240\text{--}555\text{ °C}$ temperature range, respectively. In oxygen atmosphere, APIBPOSS exhibited a two-step oxidation process in the $157\text{--}400\text{ °C}$ temperature range, whereas APIOPOSS showed a single step in the $225\text{--}445\text{ °C}$ temperature range. PIBPOSS-PCL-PIBPOSS and PIOPOSS-PCL-PIOPOSS showed two-step oxidation process in the temperature range falling in the $290\text{--}545\text{ °C}$ and $230\text{--}560\text{ °C}$ temperature range, respectively (Figs. 16,17). In nitrogen atmosphere, the pure POSS exhibited lower thermal stability compared to PCL (Fig. 14). In oxygen, APIBPOSS exhibited lower thermal stability than PCL, whereas APIOPOSS exhibited higher thermal stability than the homopolymer (Fig. 16).

The solid residue obtained from the degradations of APIBPOSS and APIOPOSS appears because of the formation of silica, SiO_2 ^{43,44} and higher residue appeared in oxygen than in nitrogen as expected.^{43,44}

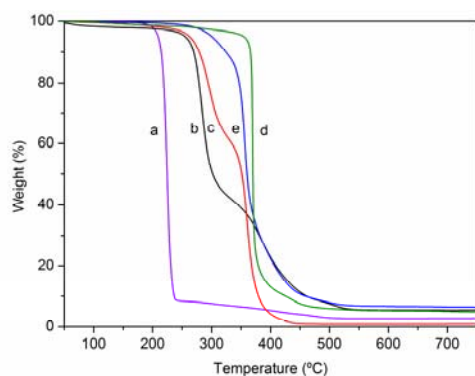


Fig. 14 TGA curves of (a) APIBPOSS, (b) APIOPOSS, (c) PCL, (d) PIBPOSS-PCL-PIBPOSS, and (e) PIOPOSS-PCL-PIOPOSS in N₂ atmosphere.

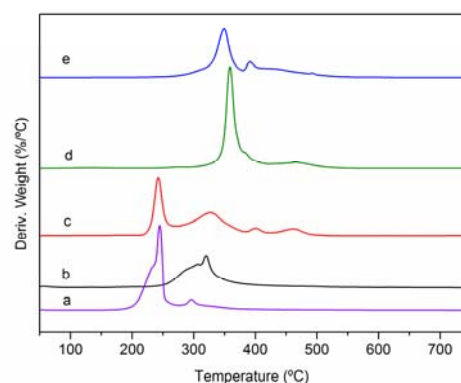


Fig. 17 DTG curves of (a) APIBPOSS, (b) APIOPOSS, (c) PCL, (d) PIBPOSS-PCL-PIBPOSS, and (e) PIOPOSS-PCL-PIOPOSS in oxygen atmosphere.

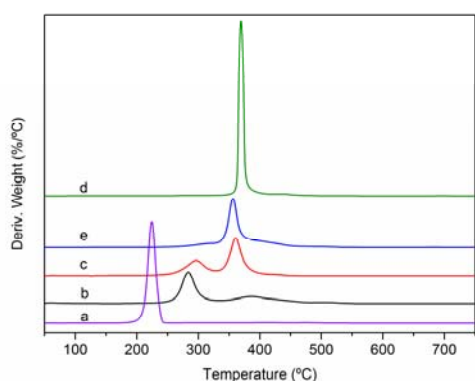


Fig. 15 DTG curves of (a) APIBPOSS, (b) APIOPOSS, (c) PCL, (d) PIBPOSS-PCL-PIBPOSS, and (e) PIOPOSS-PCL-PIOPOSS in N₂ atmosphere.

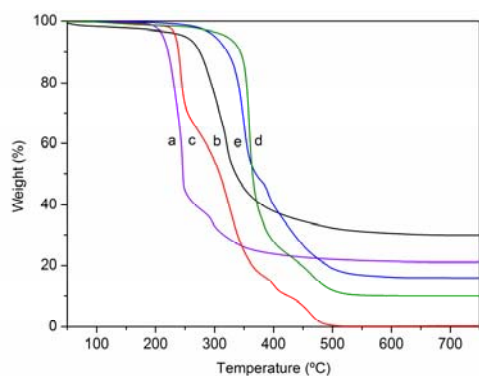


Fig. 16 TGA curves of (a) APIBPOSS, (b) APIOPOSS, (c) PCL, (d) PIBPOSS-PCL-PIBPOSS, and (e) PIOPOSS-PCL-PIOPOSS in oxygen atmosphere.

Table 2. TGA data for APIBPOSS, APIOPOSS, PCL, PLLA and telechelic hybrid

sample	T ₅ (°C)		T _{max} (°C)		Residue (%)	
	N ₂	O ₂	N ₂	O ₂	N ₂	O ₂
APIBPOSS	209	213	224	245	2.8	21.0
				296		
APIOPOSS	255	250	284	320	5.5	30.0
			388			
PCL	263	234	295	243	0.9	0
			360	327		
PIBPOSS-PCL-PIBPOSS	355	321	369	359	4.8	10.0
				465		
PIOPOSS-PCL-PIOPOSS	301	300	356	349	6.4	16.0
				392		
PLLA	220	224	239	313	0	0
PIOPOSS-PLLA	229	230	261	302	5.3	8.0

For the nanohybrids, the difference of T₅ and T_{max} values between nitrogen and oxygen atmosphere were not high. The T₅ and T_{max} values, in nitrogen and air, showed a shift to higher temperatures in the case of the hybrids compared to pure PCL, indicating higher thermal stability of the hybrids than PCL

homopolymer. For the APIBPOSS grafted sample, the T_5 value increased by about 90 °C in N_2 and oxygen compared with the PCL homopolymer. In the case of the APIOPSS grafted sample, the T_5 value increased by about 40 °C in N_2 and 65 °C in oxygen compared with the PCL homopolymer. This result was expected, since the incorporation of POSS moieties in polymer matrices would improve the thermal stability of the parent polymer due to the higher thermal stability of POSS segments.

Figs. 18 and 19 show the TG and DTG curves of APIOPSS, PLLA and PIOPOSS-PLLA in N_2 and oxygen atmosphere, respectively.

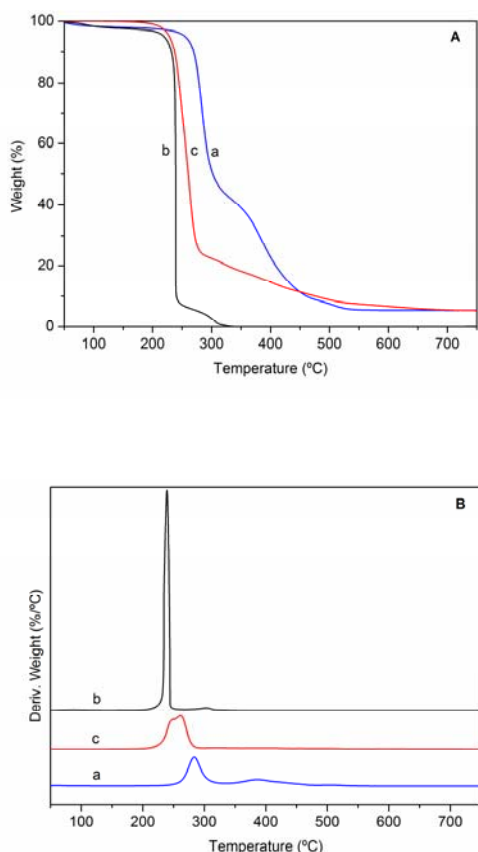


Fig. 18 TGA (A) and DTG (B) curves of (a) APIOPSS, (b) PLLA, and (c) PIOPOSS-PLLA in N_2 atmosphere.

PLLA showed a single step degradation process in N_2 atmosphere, in the 200-260 °C temperature range, whereas in oxidative atmosphere the weight loss took place in two steps in the 190-365 °C temperature range. The weight loss took place in a single step for PIOPOSS-PLLA in the two used atmosphere, falling in nitrogen in the 195-295 °C temperature range, and in oxygen in the 160-385 °C temperature range. For the PLLA and the nanohybrid, the difference of T_5 values between nitrogen and oxygen atmosphere were insignificant, while higher differences were found for the T_{max} values in the two used atmosphere, being much lower in nitrogen than under

oxygen (Table 2). A substantial solid residue was obtained from the degradations of PIOPOSS-PLLA, being higher in oxygen than in nitrogen. The T_5 and T_{max} values of PIOPOSS-PLLA, in N_2 showed a shift to higher temperatures compared to the PLLA homopolymer, indicating higher thermal stability of the hybrid than PLLA. The T_5 value of PIOPOSS-PLLA was 6 °C higher than that of PLLA in oxidative environment, while the T_{max} value of the hybrid was 11 °C lower than that of homopolymer.

The thermal decomposition of the hybrid materials were altered compared to the pure PCL and PLLA, as Figs. 14, 16, 18 and 19 demonstrate. The incorporation of the inorganic silsesquioxane cages indeed enhanced the thermal degradation properties of the nanohybrids. The higher residue for nanohybrids implied that due to the incorporation of POSS there were less volatiles released from the hybrids during heating. The lower rate of volatile release from the hybrid materials indicated enhanced flame retardancy. Therefore the inorganic component offered additional heat capacity and likely encouraged the formation of a rigid silica based shell which discouraged the existing of volatiles and decreased incoming gaseous fuel, thus stabilizing the bulk materials and discouraging thermal decomposition.

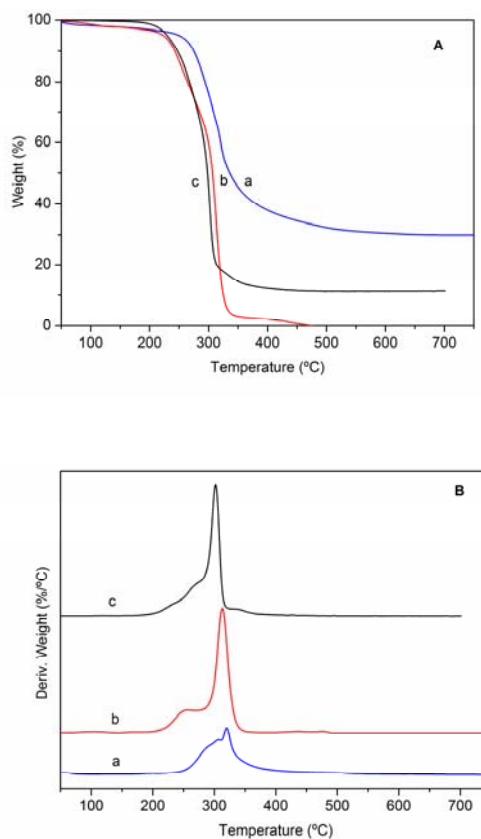


Fig. 19 TGA (A) and DTG (B) curves of (a) APIOPSS, (b) PLLA, and (c) PIOPOSS-PLLA in oxygen atmosphere.

3.3. Surface Properties

The surface properties of the organic-inorganic hybrid materials were examined in terms of the measurement of static water contact angles (WCA). The measurements were repeated 10 times in different locations on a given film, and the average values of static contact angles are presented in Table 3, while Fig. 20 shows the digit images of the WCAs for different materials.

Table 3 Contact angles of PCL, PLLA and hybrid PCL and PLLA

Sample	WCA
PCL	60.58±1.84
PIBPOSS-PCL-PIBPOSS	96.36±1.92
PIOPOSS-PCL-PIOPOSS	97.09±0.74
PLLA	76.77±1.43
PIOPOSS-PLLA	98.67±0.76
PLLA/APIOPOSS 1wt%	94.37±1.23
PLLA/APIOPOSS 2 wt%	96.21±0.70
PLLA/APIOPOSS 5 wt%	99.67±0.93

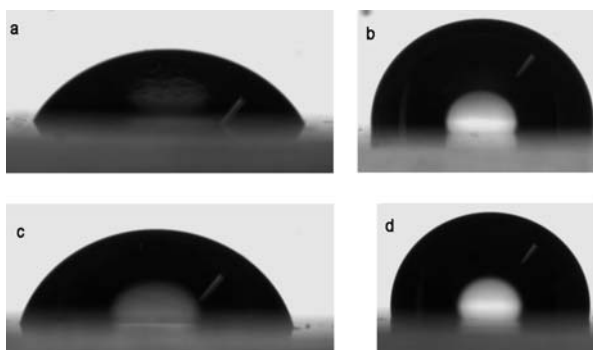


Fig. 20 Digital images of water contact angle of (a) PCL, (b) PIBPOSS-PCL-PIBPOSS, (c) PLLA, and (d) PIOPOSS-PLLA.

The incorporation of POSS gave rise to a significant increase of static WCA of PCL from 60° to about 97°. Similarly, the static WCA of PLLA increased from 77° to 99° when POSS was incorporated into PLLA chains. This increment of contact angle can be ascribed to the hydrophobic nature of

silsesquioxane molecules grafted to the polymer chains. Incorporation of POSS nanoparticles, which enhanced the water contact angles, gave rise to the improvement of the surface hydrophobicity of the materials that can be explained taking into account the effect of the seven hydrophobic isobutyl or isooctyl groups, attached to the POSS cage.

WCA of PLLA/APIOPOSS blends were also determined. The contact angles increased with increasing the content of APIOPOSS. From Table 3, it can be seen that the nanohybrid PIOPOSS-PLLA and the blend containing 5 wt% of POSS exhibited similar WCA values.

4. Conclusions

In this work, heptaisooctyl POSS-capped poly(L-lactic acid) (PLLA) telechelic, heptaisooctyl POSS-capped poly(ϵ -caprolactone) di-telechelic and heptaisobutyl POSS-capped poly(ϵ -caprolactone) di-telechelic were synthesized to obtain the organic-inorganic hybrids. The organic-inorganic hybrids were successfully obtained via click chemistry. For the click chemistry approach the alkyne-functional POSS and azide functional PLLA and PCL were used. The covalent attachment of POSS nanoparticles on the polymer chains was verified by FTIR, ^1H and ^{13}C NMR. The DSC and TGA studies demonstrated that the incorporation of POSS altered the thermal properties of PCL and PLLA. DSC results showed that the POSS-containing polymers have increased glass transition temperature. In telechelic PIBPOSS-PCL-PIBPOSS hybrid polymer both components have been found to crystallize, POSS crystallized before PCL crystallization, and the crystal formation of POSS confined the PCL crystallization, hindering the crystal formation of PCL. The incorporation of POSS disrupted the crystallization of PCL and PLLA. TGA showed that the thermal and thermoxidative stability and the yields of the degradation residues of the polymer matrices were significantly enhanced by the introduction of POSS. The static contact angle measurements showed that compared to PCL and PLLA homopolymers, the organic-inorganic hybrids displayed increased surface hydrophobicity.

Acknowledgments

The authors gratefully acknowledge the financial support by Gobierno Vasco (SAIOTEK 2012 S-PE12UN006) and the Universidad del País Vasco (UFI11/56). M. Cobos gratefully acknowledges Gobierno Vasco for a grant.

Notes and references

1. J. Wu, P.T. Mather, *J. Macromol. Sci. C Polymer Reviews*, 2009, **49**, 25–63.
2. E.T. Kopesky, T.S. Haddad, R.E. Cohen, G.H. McKinley, *Macromolecules*, 2004, **37**, 8992–9004.
3. B. Janowski, K. Pielichowski, *Polymer*, 2008, **53**, 87–98.
4. G. Li, L. Wang, H. Ni, C.U. Pittman, *J. Inorg. Organomet. Polymer*, 2001, **11**, 123–54.
5. W. Zhang, A.H.E. Müller, *Prog. Polym. Sci.*, 2013, **38**, 1121–1162.

6. K. Pielichowski, J. Njuguna, B. Janowski, J. Pielichowski, *Adv. Polym. Sci.*, 2006, **201**, 225-296.
7. J.D. Lichtenhan, *Comments. Inorg. Chem.*, 1995, **17**, 115-130.
8. J.D. Lichtenhan, Y.A. Otonari, M.J. Carr, *Macromolecules*, 1995, **28**, 8435-8437.
9. K.G. Williams, S.P. Gido, E.B. Coughlin, in *Applications of Polyhedral Oligomeric Silsesquioxanes*, ed. C. Hartmann-Thompson, Springer, New York, 2011, ch. 4, pp. 167-207.
10. J.H. Lee, Y.G. Jeong, *J. Appl. Polym. Sci.*, 2010, **115**, 1039-46.
11. W.B. Zhang, Y.W. Li, X.P. Li, X.H. Dong, X.F. Yu, C.L. Wang, C. Wesdemiotis, R.P. Quirk, S.Z.D. Cheng, *Macromolecules*, 2011, **44**, 2589-96.
12. A.L. Goffin, E. Duquesne, J.M. Raquez, H.E. Miltner, X. Ke, M. Alexandre, G. Van Tendeloo, B. Van Mele, P. Dubois, *J. Mater. Chem.*, 2010, **20**, 9415-9422.
13. T.S. Haddad, B.D. Viers, S.H. Phillips, *J. Inorg. Organomet. Polym.*, 2001, **11**, 155-164.
14. J. Wu, T.S. Haddad, G. Kim, P.T. Mather, *Macromolecules*, 2007, **40**, 544-554.
15. H. Xu, B. Yang, J. Wang, S. Guang, C. Li, *Macromolecules*, 2005, **38**, 10455-10460.
16. J. Pyun, K. Matyjaszewski, *Chem. Mater.*, 2001, **13**, 3436-48.
17. K. Ohno, S. Sugiyama, K. Koh, Y. Tsujii, T. Fukuda, M. Yamahiro, H. Oikawa, Y. Yamamoto, N. Ootake, K. Watanabe, *Macromolecules*, 2004, **37**, 8517-22.
18. W. Zhang, L. Liu, X. Zhuang, X. Li, J. Bai, Y. Chen, *J. Polym. Sci. Pol. Chem.*, 2008, **46**, 7049-61.
19. W.A. Zhang, B. Fang, A. Walther, A.H.E. Müller, *Macromolecules*, 2009, **42**, 2563-9.
20. K.M. Kim, Y. Ouchi, Y. Chujo, *Polym. Bull.*, 2003, **49**, 341-348.
21. D.B. Drzakowski, A. Lee, T.S. Haddad, D.J. Cookson, *Macromolecules*, 2006, **39**, 1854-1863.
22. C. Pan, in *Physical properties of polymers handbook*, ed. J. Mark, Springer, New York, 2007, vol. 6, pp. 577-84.
23. W.H. Binder, R. Sachsenhofer, *Macromol. Rapid Commun.*, 2007, **28**, 15-54.
24. G.W. Goodall, W. Hayes, *Chem. Soc. Rev.*, 2006, **35**, 280-312.
25. B. A. Laurent, S.M. Grayson, *J. Am. Chem. Soc.*, 2006, **128**, 4238-4239.
26. J.E. Moses, A.D. Moorhouse, *Chem. Soc. Rev.*, 2007, **36**, 1249-1262.
27. V.V. Rostovtsev, L.G. Green, V.V. Fokin, K.B. Sharpless, *Angew. Chem. Int. Ed.*, **2002**, *41*, 2596-2599.
28. H.C. Kolb, M.G. Finn, K.B. Sharpless, *Angew. Chem. Int. Ed.*, 2001, **40**, 2004-2021.
29. W.A. Zhang, A.H.E. Müller, *Macromolecules*, 2010, **43**, 3148-52.
30. M. Vert, S.M. Li, G. Spenlehauer, P. Guerin, *J. Mater. Sci -Mater. Med.*, 1992, **3**, 432-446.
31. M. Mochizuki, M. Hiram, *Polym. Adv. Technol.*, 1997, **8**, 203-209.
32. M.A. Woodruff, D.W. Hutmacher, *Prog. Polym. Sci.*, 2010, **35**, 1217-1256.
33. D. Garlotta, *J. Polym. Environ.*, 2001, **9**, 63-84.
34. Y.R. Kannan, H.J. Salacinski, P.E. Butler, A.M. Seifalian, *Acc., Chem., Res.*, 2005, **38**, 879-884.
35. R.Y. Kannana, H.J. Salacinskia, M. Odlyhab, P.E. Butler, A.M. Seifalian, *Biomaterials*, 2006, **27**, 1971-1979.
36. Y. Ni, S. Zheng, *J. Polym. Sci., Part B: Polym. Phys.*, 2007, **45**, 2201-2214.
37. Y. Ni, S. Zheng, *Macromolecules*, 2007, **40**, 7009-7018.
38. W. Kai, L. Hua, T. Dong, P. Pan, B. Zhu, Y. Inoue, *Macromol. Chem. Phys.*, 2008, **209**, 1191-1197.
39. K.M. Lee, P.T. Knight, T. Chung, P.T. Mather, *Macromolecules*, 2008, **41**, 4730-4738.
40. A.L. Goffin, E. Duquesne, S. Moins, M. Alexandre, P. Dubois, *Eur. Polym. J.*, 2007, **43**, 4103-4113.
41. J.H. Lee, Y.G. Jeong, *J. Appl. Polym. Sci.*, 2010, **115**, 1039-1046.
42. Y. Yoshida, Y. Sakakura, N. Aso, S. Okada, Y. Tanabe, *Tetrahedron*, 1999, **55**, 2183-2192.
43. A. Fina, D. Tabuani, F. Carniato, A. Frache, E. Boccaleri, G. Camino, *Thermochim. Acta.*, 2006, **440**, 36-42.
44. I. Blanco, L. Abate, F. A. Bottino, P. Bottino, *J. Therm. Anal. Calorim.*, 2012, **108**, 807-815.

Departamento de Ciencia y Tecnología de Polímeros, Facultad de Química, Universidad del País Vasco (UPV/EHU), Paseo Manuel Lardizábal 3, 20018 San Sebastián, Spain Fax: 34 943015270; Tel: 34 943015353; E-mail: mjesus.fernandez@ehu.es, mariadolores.fernandez@ehu.es, monica.cobos@ehu.es